A Comparison of Mechanical Properties of Three MEMS Materials - Silicon Carbide, Ultrananocrystalline Diamond, and Hydrogen-Free Tetrahedral Amorphous Carbon (Ta-C)

H. D. Espinosa, B. Peng and N. Moldovan, *Northwestern University, Evanston, IL 60208, USA*
T.A. Friedmann, *Sandia National Laboratories, Albuquerque, NM 87185, USA.*
X. Xiao, D.C. Mancini, O. Auciello, J. Carlisle, *Argonne National Laboratory, Argonne, IL 60439, USA*
C.A. Zorman, *Case Western Reserve University, Cleveland, OH 44106, USA*

ABSTRACT

Many MEMS devices are based on polysilicon because of the current availability of surface micromachining technology. However, polysilicon is not the best choice for devices where extensive sliding and/or thermal fields are applied due to its chemical, mechanical and tribological properties. In this work, we investigated the mechanical properties of three new materials for MEMS/NEMS devices: silicon carbide (SiC) from Case Western Reserve University (CWRU), ultrananocrystalline diamond (UNCD) from Argonne National Laboratory (ANL), and hydrogen-free tetrahedral amorphous carbon (ta-C) from Sandia National Laboratories (SNL). Young's modulus, characteristic strength, fracture toughness, and theoretical strength were measured for these three materials using only one testing methodology – the Membrane Deflection Experiment (MDE) developed at Northwestern University. The measured values of Young's modulus were 430GPa, 960GPa, and 800GPa for SiC, UNCD, and ta-C, repectively. Fracture toughness measurments resulted in values of 3.2, 4.5, and 6.2 $MPa \times m^{1/2}$, respectively. The strengths were found to follow a Weibull distribution but their scaling was found to be controlled by different specimen size parameters. Therefore, a cross comparison of the strengths is not fully meaningful. We instead propose to compare their theoretical strengths as determined by employing Novozhilov fracture criterion. The estimated theoretical strength for SiC is 10.6GPa at a characteristic length of 58nm, for UNCD is 18.6GPa at a characteristic length of 37nm, and for ta-C is 25.4GPa at a characteristic length of 38nm. The techniques used to obtained these results as well as microscopic fractographic analyses are summarized in the article. We also highlight the importance of characterizing mechanical properties of MEMS materials by means of only one simple and accurate experimental technique.

1. INTRODUCTION

Polysilicon has been the dominant material used in MEMS devices for the past ten years. As MEMS technology grows, the properties of polysilicon are becoming a limiting factor in high performance MEMS devices, particularly in harsh environments. In order to take on new challenges, new materials with attractive mechanical, electrical, and tribological properties such as silicon carbide (SiC), ultrananocrystalline diamond (UNCD), and hydrogen-free tetrahedral amorphous carbon (ta-C) have emerged. SiC has been a favorable alternate material because of its high temperature stability, relatively high stiffness and strength. It has been used in high temperature sensors, micro power applications, and some bio-MEMS. However, SiC has some tribological shortcomings as identified in MEMS devices [1]. UNCD and ta-C are ultrahard materials with high stiffness, high fracture strength and toughness, exceptional chemical inertness and outstanding wear resistance among other properties [2-4]. Some of their mechanical properties, such as elastic modulus and fracture strength, are close to those of single-crystal diamond. Moreover, it has been demonstrated that standard microfabrication techniques can be employed to manufacture functional structures and devices made of UNCD and ta-C.

With the increasing demands in design and fabrication of MEMS/NEMS devices out of SiC, UNCD, and ta-C, the need for accurate characterization of their mechanical properties at scales of relevance is a high priority in the MEMS community. Advancements in mechanical testing has enabled the characterization of Young's modulus, Poisson's ratio, fracture toughness, and strength size dependence for a variety of materials in the form of thin films. However, the results varied for different testing techniques. In this work, we report a comparison of the properties of these relatively new MEMS materials based on a *sole* experimental technique.

SiC, UNCD, and ta-C are materials displaying a linear stress-strain response up to fracture. Their fracture strengths are not a constant value but rather a statistical parameter. The distribution of their strengths was found to follow Weibull statistics [5-7]. However, the scaling parameter was found to be

highly dependent on the material system and film fabrication technique. In this regards, a comparison of strengths between MEMS materials, in terms of the two Weibull parameters - modulus and characteristic strength, becomes relevant only if the scaling parameter, e.g., volume or sidewall area, is the same. In addition to strength, fracture toughness K_{IC} is another important parameter in some engineering applications because it is a measure of the material resistance to crack growth from a pre-existing defect. K_{IC} depends only on material micro structural features and it is independent of specimen geometry, boundary conditions and loading. Consequently, one way to compare structures of different geometries is on the basis of their respective stress intensity levels [8]. Recently, Pugno *et al*. [9] proposed a new approach to estimate the ideal or theoretical strength, σ_u, of the material at a characteristic length, d_0. The estimation is based on the measurement of the stress intensity level at sharp cracks and blunt notches. It turns out that σ_u and d_0 are material parameters that give a direct indication of the material ultimate strength at a characteristic length scale.

In this paper, we use the membrane deflection experiment (MDE) developed at Northwestern University to investigate and compare these mechanical properties, Young's modulus, characteristic strength and Weibull modulus associated to a scaling parameter (volume, surface area, or sidewall area), fracture toughness, and ideal strength at a characteristic dimension, for three MEMS materials: SiC from Case Western Reserve University (CWRU), ta-C from Sandia National Laboratories (SNL), and UNCD from Argonne National Laboratory (ANL).

2. EXPERIMENTAL PROCEDURE

2.1. Materials

The SiC from Case Western Reserve University is a polycrystalline film deposited in a hot-wall, rf-induction-heated, low-pressure chemical vapor deposition (LPCVD) furnace. The growth procedure involves SiH_2Cl_2/C_2H_2 as reacting gases with pressure in the range of 460 and 510 mTorr at a temperature of about 900^{o}C. The film is polycrystalline with columnar grains approximately 200 nm in size [10]. Deposition of UNCD films was performed in a 6" Cyrannus-IPLAS (Innovative Plasma Systems GmbH) reactor at 800^{o}C by employing microwave pressure enhanced chemical vapor deposition (MPECVD). This process utilizes argon rich CH_4/Ar plasma chemistries [11], where C_2 dimers are the growth species derived from collision induced fragmentation of CH_4 molecules in an Ar plasma. The UNCD film consists of crystalline grains, 95% sp^3 bonded carbon, with an average grain size of 3-5nm. The stress-free ta-C film was deposited at SNL at room temperature via pulsed laser deposition (PLD) [4] and annealed at 600-650 ^{o}C to relieve the high residual stress. The ta-C film contains a mixture of roughly 80% sp^3/20% sp^2 with very little hydrogen (<1%).

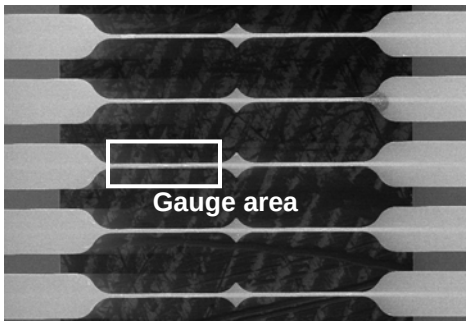

Figure1: SEM image of the specimens.

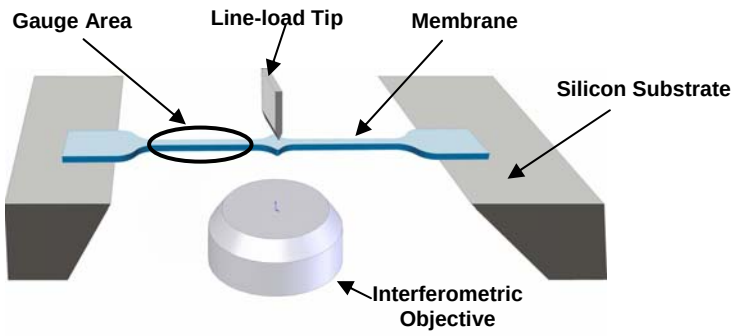

Figure 2: Schematic drawing of the MDE setup.

The microfabrication of the membrane deflection tensile specimens is similar for the three hard materials. 4" inch wafers with one side polished and the other side coated by low stress Si_3N_4 were sent out to CWRU, ANL, and SNL for film deposition. All the wafers were cleaned using standard RCA cleaning process before deposition. The films were patterned and etched by oxygen plasma etching using a E-beam deposited aluminum (300nm thick) as a mask. The gauge section is released by etching the underlying silicon wafer with KOH. Fig. 1 shows a SEM image of the microfabricated SiC specimen. The geometry of the membrane is such that it contains tapered regions to eliminate boundary failure effects (Fig.1). The

membrane is attached at both ends and spans a micromachined window beneath. Several sizes of membrane specimens were designed on a single wafer to examine size scale effects.

2.2 Tensile Testing

The Membrane Deflection Experiment (MDE) developed by Espinosa *et al*. [12] was used to deform and stress the specimens until failure. A combined Nanoindenter and Atomic Force Microscope (AFM) apparatus was used in this investigation to apply a line load to the center of the membranes (Fig. 2). The procedure involves applying a line-load at the center of the spanning membrane. Simultaneously, an interferometer focused on the bottom side of the membrane records the deflection. The result is direct tension with load and deflection being measured independently. A calibration plot, experimental details, and formulas used to compute stress and strain can be found in [12].

Table 1: Measured elastic modulus and fracture strengths for the three tested materials.

Material	SiC		UNCD		Ta-C	
	Size A	Size B	Size A	Size B	Size A	Size B
No. of tests	30	30	30	30	30	30
Thickness (nm)	855±53	527±29	1050±77	515±21	896±33	501±12
Young's modulus (GPa)	422±18	435±15	960±25	955±21	801±22	795±34
Fracture strength (MPa)	2090 ±519	2680 ±556	3990 ±428	5080±555	4680±540	5260±459
Weibull modulus	5.4±0.27		11.6±0.58		12.0±0.60	
σ_{0V} or σ_{0A}	6780±339 [(MPa×(μm)$^{2/m}$]		8560±428 [(MPa×(μm)$^{3/m}$]		8020±401 [(MPa×(μm)$^{2/m}$]	
Controlling factor	Sidewall		Volume		Sidewall	

3. RESULTS AND DISCUSSIONS

3.1 Young's Modulus and Characteristic Strengths

The thickness of the films was measured by atomic force microscopy (AFM) before testing and also by SEM after the specimens were broken. Thirty tests for each specimen size, size A (20μm wide and 200μm long) and size B (5μm wide and 100μm long), were performed under the same conditions using the MDE technique. Results for elastic modulus and strength were found for each material as seen in table 1 (Rows 4 –6).

3.1.1 Weibull Analysis

All the materials exhibited strengths dependent on the specimen size, with the smallest specimen exhibiting the highest fracture strength. However, whether the strength scales with volume, surface, or sidewall area is not known. The widely used Weibull statistics allows examination of strength values in the sense of failure probability at a certain stress level. In particular, Weibull's theory is capable of predicting the materials strength as a function of the sample sizes (the applicability of the theory to MEMS materials was verified by Bagdahn *et al*. [6] and Peng *et al*. [7]). To take into account the effect of volumes or areas the probability of failure is written as:

$$P_f = 1 - \exp\left[-\left(\frac{\sigma_{\max}}{\sigma_{0V}}\right)^m V_e\right], \text{ or } P_f = 1 - \exp\left[-\left(\frac{\sigma_{\max}}{\sigma_{0A}}\right)^m A_e\right] \quad (1)$$

where σ_{0V} and σ_{0A} are strengths relative to unit size (characteristic strength), and V_e or A_e is the effective volume or area of the samples subjected to uniform stress. σ_{0V} and σ_{0A} have the units of MPa×(meters)$^{3/m}$ or MPa×(meters)$^{2/m}$. If the uniaxial Weibull model described above is valid, then the two parameters, m and σ_{0V} (σ_{0A}), are material constants. Given the dimenstions of the uniaxial gauge section the two Weibull parameters can be estimated from the experimentally measured failure stress, $\sigma_{\max}$, by nonlinear regression [13]. Since the fracture strength of brittle materials depends on size, it is useful to test specimens with different sizes and to "pool" those results into one single large data set to improve the statistical accuracy. Fig. 3 shows the estimated characteristic strengths, σ_{0V} and σ_{0A}, based on specimens' volume, total surface area, and sidewall area. If the characteristic strength is constant, by fitting the experimental data with Eq. 1, we should get the same value of σ_{0V} (σ_{0A}) for any size sample. In Fig. 3 we compare the characteristic strengths of size A and size B samples with the pooled value. For SiC, it is found that σ_{0A} estimated from

sidewall area has the smallest scattering for different sizes indicating that the strength scales with sidewall area. Similarly, for ta-C the strength also scales with sidewall area. By contrast, the UNCD strength is found to scale with volume.

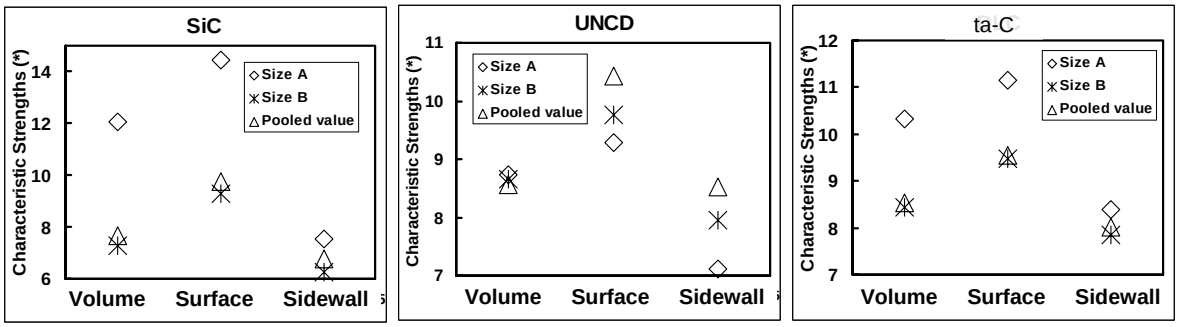

Figure 3: The estimated Weibull scale parameters based on volume, total surface area, and sidewall area. (*σ_{0V} and σ_{0A} have the peculiar units of GPa×(μm)$^{3/m}$ or GPa×(μm)$^{2/m}$).

Knowing the Weibull modulus, the characteristic strength, and the scaling parameter (Table 1, Rows 7 – 9), different sets of data can be transformed into one single data with respect to unit size (see Fig. 4).

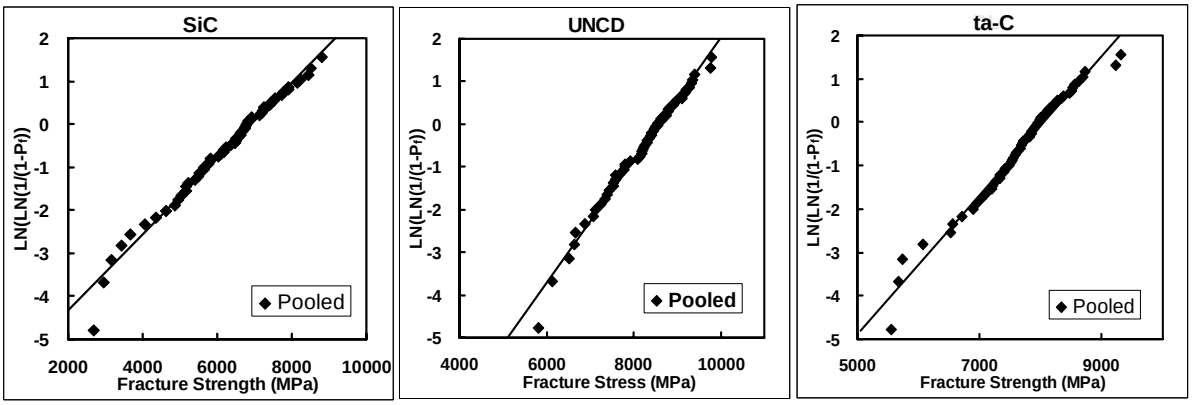

Figure 4: Weibull plots showing fracture strength transformed to unit size in uniaxial tension. SiC and ta-C are transformed to unit sidewall area and UNCD is transformed to unit volume.

3.1.2 Fractrographic Analysis

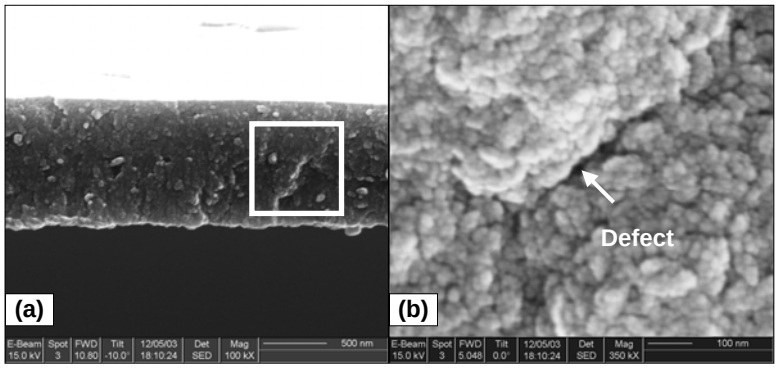

Figure 5: (a) Overview of the fracture surface of a UNCD specimen and (b) magnified view of the area within the white rectangle. The arrow in (b) points to a defect in the bulk of the specimen.

The fracture surfaces were examined with a high resolution FEG-SEM. Fig. 5 shows a typical fracture surface of an UNCD sample at two magnifications. In principle, the fracture origin could be on the sidewalls, the top or bottom surfaces, or within the volume. However, there is no evidence of fracture initiation at the surface area or the sidewall as was found for poly-silicon [6]. Fig. 5 shows that fracture most likely initiates from interior defects introduced during the film deposition process. Fig. 5b reveals that the grooves observed in Fig. 5a are actually clusters of grains. It is clear from these images that intergranular failure dominates the failure process in the tested UNCD films.

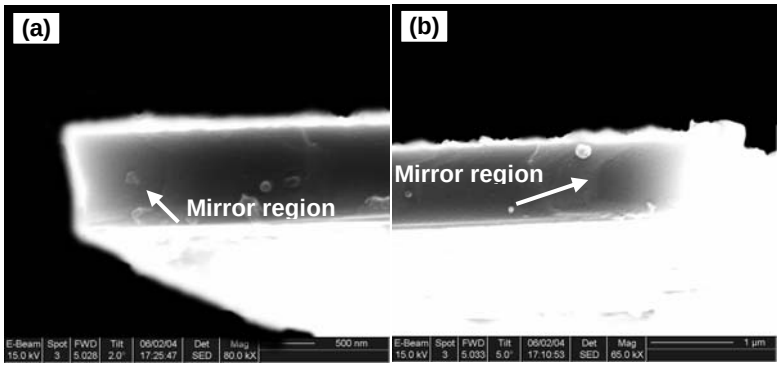

Figure 6: (a) Fracture surface of a ta-C specimen and (b) SiC specimen. The arrows point to mirror regions where the failures originate.

Fig. 6a is a typical fracture surface of ta-C. As expected from the amorphous structure the fracture surface is smoother when compared to that of UNCD. There is a "mirror" region at the edge of the sidewall. This feature is perpendicular to the maximum tensile direction and its front is approximately circular. These images confirm that the sidewall roughness can act to concentrate stress and is the origin of fracture. The fracture surface of SiC is similar to that of ta-C (Fig. 6b). Hence, the failure origins for ta-C and SiC are found to be the sidewall, which is consistent with the identified scaling parameters based solely on statistics.

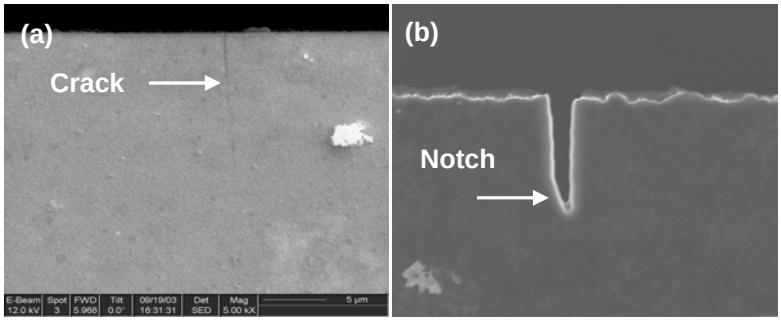

Figure 7: (a) SEM micro graph showing a sharp crack induced from an indent, (b) a blunt notch produced by focused ion beam in a UNCD sample.

3.2. Fracture Toughness and Ideal Strength

The fracture toughness, K_{IC}, can be determined using the membrane deflection technique by stretching specimens possessing sharp cracks [14]. Sharp cracks were achieved by placing a Vickers indent and emanating corner cracks (at maximum load of 200g) near the specimen prior to the film release. Although the indent was placed on the silicon substrate the radial crack initiated at one of the corners of the indent propagated into the specimen. The length of the crack was measured using high-resolution scanning electron microscope (SEM), see Fig. 7a. In this configuration (edge crack), the fracture toughness can be computed from the following equations:

$$K_{IC} = \sigma_f \sqrt{\pi a}\, f\left(\frac{a}{W}\right) \tag{2}$$

$$f\left(\frac{a}{W}\right) = 1.12 - 0.23\left(\frac{a}{W}\right) + 10.55\left(\frac{a}{W}\right)^2 - 21.72\left(\frac{a}{W}\right)^3 + 30.41\left(\frac{a}{W}\right)^4 \tag{3}$$

where σ_f is the failure stress, a is the length of the crack and W is the width of the gauge region. The constraint $a/W \le 0.6$ applies. Alternatively, blunt notches with finite tip radii were fabricated using focused ion beam (FIB) micro milling (Fig. 7b) [14]. The equivalent stress-intensity factor, K'_{IC}, from a blunt notch can be computed by:

$$K'_{IC} = \sqrt{1 + \frac{\rho}{2d_0}}\, K_{IC} \tag{4}$$

in which ρ is the root notch radius and the finite length d_0 is a characteristic dimension derived in [9] and given by:

$$d_0 = \frac{2}{\pi}\frac{K_{IC}^2}{\sigma_u^2} \tag{5}$$

In this equation, σ_u is the ideal or theoretical strength of the material at the characteristic length of d_0. Note that d_0 can be obtained by matching two different experimental results performed on notches with different

root radii ρ, as suggested by Eq. (4). In this work we matched the experimental results corresponding to values of ρ = 100 nm and 200 nm.

Five specimens for each material with sharp cracks were tested under the same condition except that the crack length, *a*, was varied. The fracture toughness was computed using Eq. (2) and was found to be independent of the crack length. This confirms that only the region of the material immediately in front of the pre-crack affects the material toughness. The measured fracture toughness, equivalent stress-intensity factor of a blunt notch, and the computed ideal strength are presented in table 2.

Table 2: Measured fracture toughness, equivalent stress-intensity factors, and ideal strengths.

Material	K_{IC} [MPa $\sqrt{\text{m}}$]	K'_{IC} [MPa $\sqrt{\text{m}}$]	d_0 [nm]	σ_u [GPa]
SiC	3.2	5.3 (ρ=200nm)	58	10.6
UNCD	4.5	6.9 (ρ=100nm)	37	18.6
ta-C	6.2	11.8 (ρ=200nm)	38	25.4

4. CONCLUSIONS

In this work, we used the membrane deflection experiment (MDE) to measure the mechanical properties of SiC, UNCD, and ta-C. The specimens were microfabricated using similar cleanroom processes. Freestanding membranes with thicknesses in the range of 500-1000 nm were fabricated and tested. The measured values of Young's modulus are 430GPa, 960GPa, and 800GPa for SiC, UNCD, and ta-C, repectively. For all the materials, the fracture strengths were found to be decreasing with increasing specimen sizes. However, the scaling parameters were found to be material microstructure and frabrication-induced roughness. For UNCD the scaling parameter was found to be volume, while for ta-C and SiC it was found to be sidewall area. The Weibull modulii were estimated to be 5.4, 11.6, and 6.2 GPa; the characteristic strengths were 6.8GPa×(μm)$^{2/m}$, 8.6GPa×(μm)$^{3/m}$, and 8.0GPa×(μm)$^{2/m}$ for SiC, UNCD, and ta-C, repectively. The results show that Ta-C has the highest fracture toughness, 6.2 MPa m$^{1/2}$, and theoretical strength, 25.4GPa.

5. ACKNOWLEDGEMENTS

We would like to thank N. Pugno for many insightful suggestions concerning the identification of material theoretical strength. The authors would like to acknowledge the contributions of R.S. Divan (ANL) in the microfabrication of the tensile specimens and I. Petrov, J. Mabon and M. Marshall, from the microscopy research lab at UIUC, for their assistance in the SEM observations. The work at Northwestern University was supported in part by the NSF-Nano Science Interdisciplinary Research Teams (NIRT) under Award Number CMS-00304472 and by the National Science Foundation under GOALI Award No. CMS-0120866/001. The work at SNL was supported by Sandia Corporation, a Lockheed Martin Company, for the U.S. Department of Energy's National Nuclear Security Administration under contract DE-AC04-94AL85000. The work at Argonne National Laboratory was supported by the office of Science, Basic Energy Sciences, under Contract Number W-31-109-ENG-38. This work is also supported in part by the DOE Center of Excellence for the Synthesis and Processing of Advanced Materials.

REFERENCE

1. A.P. Lee, A.P. Pisano, M.G. Lim, 1992 *Mater. Res. Soc. Symp. Proc.* **276** 67
2. Auciello, J. Birrell, J.A. Carlisle, J.E. Gerbi, X. Xiao, B. Peng, H.D. Espinosa, 2004 *J. Phy.* **16** 539
3. J.P. Sullivan, T.A. Friedmann, M.P. de Boer, D.A. LaVan, R.J. Hohlfelder, C.I.H. Ashby, M.T. Dugger, M. Mitchell, R.G. Dunn, A.J. Magerkurth, 2001 *Mat. Res. Soc. Symp. Proc.* **657** EE7.1.1
4. J.P. Sullivan, T.A. Friedmann, K. Hjort, 2001 *MRS Bulletin* **26** 309
5. T. E. Buchheit, S. J. Glass, J. R. Sullivan, S. S. Mani, D. A. Lavan, T. A. Friedmann, R. Janek, 2003 *J. Mater. Sci.* **38** 4081
6. J. Bagdahn, W.N. Sharpe, O. Jadaan, 2003 *J. MEMS* **12** 302
7. B. Peng, H.D. Espinosa, N. Moldovan, X. Xiao, O. Auciello, J.A. Carlisle, 2004 submitted to *J. Appl. Phy.*
8. R.W. Hertzberg, 1996 *Deformation and Fracture Mechanics of Engineering Materials* 315
9. N. Pugno, B. Peng, H.D. Espinosa, 2004 in press *Int. J. Solids and. Struc.*
10. C.A. Zorman, S. Rajgopal, X.A. Fu, R. Jezeski, J. Melzak, M. Mehregany, 2002 *Elec. Chem. Sol. Lett.* **5** G99
11. D.M. Gruen, 1999 *Ann. Rev. Mat. Sci* **29** 211
12. H.D. Espinosa, B.C. Prorok, M. Fischer, 2003 *J. Mech. Phy. Sol.* **51** 47
13. C.A. Johnson, W.T. Tucker, 1991 *Engineered Materials Handbook* **4** 709
14. H.D. Espinosa, B. Peng, 2004 in press *J. MEMS*